Silica-Based Nanohybrids Containing Dipyridine, Urethan, or Urea Derivatives

Sandra Cousinié, Marie Gressier, Pierre Alphonse, and Marie-Joëlle Menu*

Centre Interuniversitaire de Recherche et d'Ingénierie des Matériaux, UMR-CNRS 5085, Université Paul Sabatier, 118 route de Narbonne, 31062 Toulouse Cedex 9, France

Received July 18, 2007. Revised Manuscript Received September 17, 2007

New nanohybrids were synthesized by grafting organosilanes on silica nanoparticles. These nanohybrids containing dibipyridine, urea, and urethan functionalities can be used as new synthons for nanotechnology, catalysis, or nanocomposites. The influence of the organosilane amount was studied together with the pH and solvent effects. The nanohybrids have been thoroughly characterized by diffuse reflectance IR Fourier transform (DRIFT) and NMR spectroscopies, electron microscopy (transmission and scanning), thermogravimetry (thermogravimetric analysis and differential thermal analysis), and nitrogen adsorption. We have demonstrated that grafting can occur in two ways on the silica surface: organosilane oligomer grafting or organosilane monolayer grafting. Through the synthesis of new organosilanes, containing dipyridine functionality combined with methylaminopropylsilane, interesting electronic and complexing properties are now available on the silica surface for further reactivity. This has been obtained for both triethoxysilyl and dimethylethoxysilyl derivatives with the same grafting ratio indicating that dimethylethoxysilane is a good precursor for developing nanohybrid chemistry. In this case, organosilane monolayer grafted nanoparticules were ascertained. Once grafted, the chemical integrity of ureas, urethan, and dipyridine silanes were preserved, as demonstrated by DRIFT and ^{13}C cross polarization magic angle spinning (CP MAS) NMR spectroscopies, and covalent grafting on silanol sites was confirmed by ^{29}Si CP MAS NMR experiments. The size and morphology of silica nanoparticles were retained after grafting as long as the organosilane-to-silica ratio did not exceed 2 mmol g^{-1}, even in water or water/alcohol mixtures. This work demonstrates that it is possible to limit the grafting to lower oligomers, giving nanohybrids with very interesting chemical surface reactivity.

1. Introduction

The functionalization of silica particles has been the object of great interest and intensive investigation because the surface properties of silica materials are largely influenced by the nature of the surface functional groups. Functionalized silica is a versatile material, and ways to effectively introduce organic functional groups onto the surfaces[1] and insides[2] of the particles are now under control for many applications. Recently, the chemical modification of nanosized silica particles has been used in chemical sensor synthesis,[3–5] in catalysis,[6–8] and especially in the synthesis of new silica-based hybrid nanosynthons for bionanotechnology as gene and drug transfer vehicles,[9–12] luminescent probes,[11,13,14] or bioseparation.[15,16]

Interest in silica nanoparticules as tools for bionanotechnology is largely expressed by recent reviews of Tan et al.[17,18] and Wiesner et al.[19] The incorporation of magnetic compounds[20–23] or organic[24–27] or inorganic dyes[28–30] into

* Corresponding author. Tel.: (33)561558487. Fax: (33)561556163. E-mail: menu@chimie.ups-tlse.fr.

(1) Vansant, E. F.; Van der Voort, P.; Vrancken, K. C. *Characterisation and Chemical Modification of the Silica Surface*; Delmon, B., Yates, J. T., Eds.; Elsevier: Amsterdam, 1995; Studies in Surface Science and Catalysis, 93, 1st ed.
(2) Stober, W.; Fink, A.; Bohn, E. *J. Colloid Interface Sci.* **1968**, *26*, 62.
(3) Zhang, F.-F.; Wan, Q.; Wang, X.-L.; Sun, Z.-D.; Zhu, Z.-Q.; Xian, Y.-Z.; Jin, L.-T.; Yamamoto, K. *J. Electroanal. Chem.* **2004**, *571*, 133.
(4) Belyakova, L. A.; Vlasova, N. N.; Golovkova, L. P.; Varvarin, A. M.; Lyashenko, D. Y.; Svezhentsova, A. A.; Stukalina, N. G.; Chuiko, A. A. *J. Colloid Interface Sci.* **2003**, *258*, 1.
(5) Qhobosheane, M.; Santra, S.; Zhang, P.; Tan, W. *Analyst* **2001**, *126*, 1274.
(6) Kovalchuk, T.; Sfihi, H.; Kostenko, L.; Zaitsev, V.; Fraissard, J. *J. Colloid Interface Sci.* **2006**, *302*, 214.
(7) Li, Z.; Peng, Q.; Yuan, Y. *Appl. Catal., A* **2003**, *239*, 79.
(8) Bianchini, C.; Dal Santo, V.; Meli, A.; Moneti, S.; Moreno, M.; Oberhauser, W.; Psaro, R.; Sordelli, L.; Vizza, F. *J. Catal.* **2003**, *213*, 47.
(9) Luo, D.; Han, E.; Belcheva, N.; Saltzman, W. M. *J. Controlled Release* **2004**, *95*, 333.
(10) Azioune, A.; Slimane, A. B.; Hamou, L. A.; Pleuvy, A.; Chehimi, M. M.; Perruchot, C.; Armes, S. P. *Langmuir* **2004**, *20*, 3350.
(11) Hilliard, L. R.; Zhao, X.; Tan, W. *Anal. Chim. Acta* **2002**, *470*, 51.
(12) Kneuer, C.; Sameti, M.; Haltner, E. G.; Schiestel, T.; Schirra, H.; Schmidt, H.; Lehr, C.-M. *Int. J. Pharm.* **2000**, *196*, 257.
(13) Lu, C.-W.; Hung, Y.; Hsiao, J.-K.; Yao, M.; Chung, T.-H.; Lin, Y.-S.; Wu, S.-H.; Hsu, S.-C.; Liu, H.-M.; Mou, C.-Y.; Yang, C.-S.; Huang, D.-M.; Chen, Y.-C. *Nano Lett.* **2007**, *7*, 149.
(14) Lian, W.; Litherland, S. A.; Badrane, H.; Tan, W.; Wu, D.; Baker, H. V.; Gulig, P. A.; Lim, D. V.; Jin, S. *Anal. Biochem.* **2004**, *334*, 135.
(15) Smith, J. E.; Wang, L.; Tan, W. *Trends Anal. Chem.* **2006**, *25*, 848.
(16) Gu, H.; Xu, K.; Xu, C.; Xu, B. *Chem. Commun.* **2006**, 941.
(17) Wang, L.; Wang, K.; Santra, S.; Zhao, X.; Hilliard, L. R.; Smith, J. E.; Wu, Y.; Tan, W. *Anal. Chem.* **2006**, 646.
(18) Tan, W.; Wang, K.; He, X.; Zhao, X. J.; Drake, T.; Wang, L.; Bagwe, R. P. *Med. Res. Rev.* **2004**, *24*, 621.
(19) Burns, A.; Ow, H.; Wiesner, U. *Chem. Soc. Rev.* **2006**, *35*, 1028.
(20) Liu, X.; Ma, Z.; Xing, J.; Liu, H. *J. Magn. Magn. Mater.* **2004**, *270*, 1.
(21) Tartaj, P.; Serna, C. J. *J. Am. Chem. Soc.* **2003**, *125*, 15754.
(22) Levy, L.; Sahoo, Y.; Kim, K. S.; Bergey, E. J.; Prasad, P. N. *Chem. Mater.* **2002**, *14*, 3715.

10.1021/cm7019075 CCC: $37.00 © 2007 American Chemical Society
Published on Web 11/22/2007

Scheme 1. Functionalization of Silica Nanoparticles and Applications

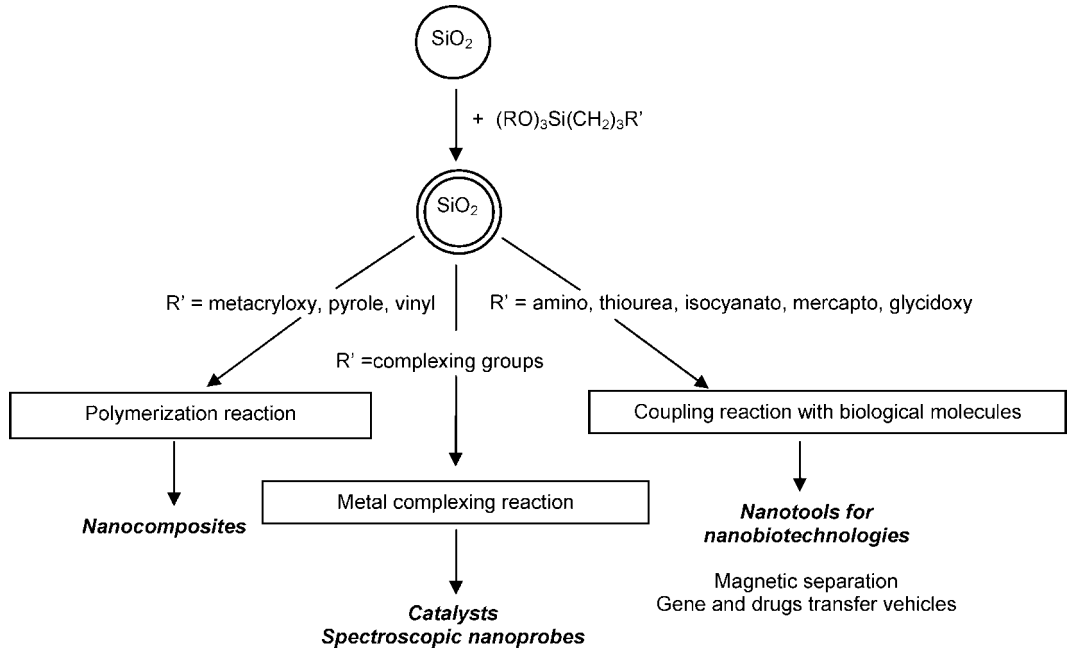

silica nanoparticles is well reported by condensation of the reactive species with tetraethoxysilane in a Stöber-type reaction[2] or a reverse microemulsion system.[31] In all of these applications, silica nanoparticles may be considered as nanobuilding blocks for which the surface has to be tailored. The nanostructure, degree of organization, and properties of the resulting organic–inorganic hybrid materials depend on and therefore may be controlled by a full knowledge of the chemical nature of the surface of these nanobuilding blocks. To synthesize them, we need bifunctional reactants containing alkoxysilylane functionalities. This is the more convenient function for a covalent grafting onto a silica surface by condensation with the surface silanols. Various reactivities may be expected according to the nature of the second functional group (Scheme 1) such as (i) polymerization reactions (metacryloxy,[32–35] pyrole,[36] and vinyl[37–39]) for application as fillers in nanocomposites,[40–43] (ii) coupling reactions with biological molecules (amino,[4,44–49] isocyanato,[50] mercapto,[51] glycidoxy,[46,52,53] or carboxyl[54,55] groups) with the aim of nanobiotechnology applications, or (iii) metallic cation complexing reactions.[56–58] If the left-hand way in Scheme 1 is satisfied with a rough organic coating as a functionalization, the right-hand and central ways need

(23) Santra, S.; Tapec, R.; Theodoropoulou, N.; Dobson, J.; Hebard, A.; Tan, W. *Langmuir* **2001**, *17*, 2900.
(24) Wang, L.; Tan, W. *Nano Lett.* **2006**, *6*, 84.
(25) Bagwe, R. P.; Yang, C.; Hilliard, L. R.; Tan, W. *Langmuir* **2004**, *20*, 8336.
(26) Yang, W.; Zhang, C. G.; Qu, H. Y.; Yang, H. H.; Xu, J. G. *Anal. Chim. Acta* **2004**, *503*, 163.
(27) Tapec, R.; Zhao, R.; Tan, W. *J. Nanosci. Nanotechnol.* **2002**, *2*, 405.
(28) Yao, G.; Wang, L.; Wu, Y.; Smith, J.; Xu, J.; Zhao, W.; Lee, E.; Tan, W. *Anal. Bioanal. Chem.* **2006**, *385*, 518.
(29) Rossi, L. M.; Shi, L.; Quina, F. H.; Rosenzweig, Z. *Langmuir* **2005**, *21*, 4277.
(30) Lian, W.; Litherland, S. A.; Badrane, H.; Tan, W.; Wu, D.; Baker, H. V.; Gulig, P. A.; Lim, D. V.; Jin, S. *Anal. Biochem.* **2004**, *334*, 135.
(31) Arriagada, F. J.; Osseo-Asare, K. *J. Colloid Interface Sci.* **1999**, *211*, 210.
(32) Posthumus, W.; Magusin, P. C. M. M.; Brokken-Zijp, J. C. M.; Tinnemans, A. H. A.; Van der Linde, R. *J. Colloid Interface Sci.* **2004**, *269*, 109.
(33) Bauer, F.; Glasel, H.-J.; Decker, U.; Ernst, H.; Freyer, A.; Hartmann, E.; Sauerland, V.; Mehnert, R. *Prog. Org. Coat.* **2003**, *47*, 147.
(34) Bauer, F.; Glasel, H.-J.; Hartmann, E.; Bilz, E.; Mehnert, R. *Nucl. Instrum. Methods Phys. Res., Sect. B* **2003**, *208*, 267.
(35) Bourgeat-Lami, E.; Espiard, P.; Guyot, A. *Polymer* **1995**, *36*, 4385.
(36) Garbassi, F.; Occhiello, E.; Bastioli, C.; Romano, G. *J. Colloid Interface Sci.* **1987**, *117*, 258.
(37) Caregnato, P.; LeRoux, G. C.; Martire, D. O.; Gonzalez, M. C. *Langmuir* **2005**, *21*, 8001.
(38) Bharali, D. J.; Kleijbor, I.; Stachowiak, E. K.; Dutta, P.; Roy, I.; Kaur, N.; Bergey, E. J.; Prasad, P. N.; Stachowiak, M. K. *Proc. Natl. Acad. Sci. U.S.A.* **2005**, *102*, 11539.
(39) Jeon, B. J.; Hah, H. J.; Koo, S. M. *J. Cer. Proc. Res.* **2002**, *3*, 216.
(40) Kim, S. H.; Ahn, S. H.; Hirai, T. *Polymer* **2003**, *44*, 5625.
(41) Ceccorulli, G.; Zini, E.; Scandola, M. *Macromol. Chem. Phys.* **2006**, *207*, 864.
(42) Malucelli, G.; Priola, A.; Sangermano, M.; Amerio, E.; Zini, E.; Fabbri, E. *Polymer* **2005**, *46*, 2872.
(43) Ding, X.; Zhao, J.; Liu, Y.; Zhang, H.; Wang, Z. *Mater. Lett.* **2004**, *58*, 3126.
(44) Liu, S.; Zhang, H.-L.; Liu, T.-C.; Liu, B.; Cao, Y.-C.; Huang, Z.-L.; Zhao, Y.-D.; Luo, Q.-M. *J. Biomed. Mater. Res., Part A* **2007**, *80*, 752.
(45) Del Campo, A.; Sen, T.; Lellouche, J. P.; Bruce, I. J. *J. Magn. Magn. Mater.* **2005**, *293*, 33.
(46) Liu, X.; Xing, J.; Guan, Y.; Shan, G.; Liu, H. *Colloids Surf., A* **2004**, *238*, 127.
(47) Horr, T. J.; Arora, P. S. *Colloids Surf., A* **1997**, *126*, 113.
(48) Van Blaaderen, A.; Vrij, A. *Langmuir* **1992**, *8*, 2921.
(49) Van Blaaderen, A.; Vrij, A. *J. Colloid Interface Sci.* **1993**, *156*, 1.
(50) Csögor, Z.; Nacken, M.; Sameti, M.; Lehr, C. M.; Schmidt, H. *Mater. Sci. Eng., C* **2003**, *23*, 93.
(51) Hilliard, L.; Zhao, X.; Tan, W. *Anal. Chim. Acta* **2002**, *470*, 51.
(52) Innocenzi, P.; Brusatin, G.; Guglielmi, M.; Bertani, R. *Chem. Mater.* **1999**, *11*, 1672.
(53) Sharma, R. K.; Das, S.; Maitra, A. *J. Colloid Interface Sci.* **2004**, *277*, 342.
(54) Markowitz, M. A.; Schoen, P. E.; Kust, P.; Gaber, B. P. *Colloids Surf., A* **1999**, *150*, 85.
(55) Deng, G.; Markowitz, M. A.; Kust, P.; Gaber, B. P. *Mater. Sci. Eng., C* **2000**, *11*, 165.
(56) de Monredon, S.; Pottier, A.; Maquet, J.; Babonneau, F.; Sanchez, C. *New J. Chem.* **2006**, *30*, 797.
(57) Verwilghen, C.; Guilet, R.; Deydier, E.; Menu, M.-J.; Dartiguenave, Y. *Environ. Chem. Lett.* **2004**, *2*, 215.
(58) Spennato, R.; Menu, M.-J.; Dartiguenave, M.; Dartiguenave, Y. *Trans. Met. Chem.* **2004**, *29*, 830.

a strictly covalent functionalization like organosilane monolayered grafting. Of course, covalent grafting guarantees the essential high stability and good homogeneity of the provided materials, but the most important aspect is presence on the surface of accessible organic functional groups for further reactivity. In this latter case, which requires our interest, the powerful reactivity of metallic species can be coupled to silicated materials to enable very interesting applications as new catalysts, more sensitive spectroscopic nanoprobes, or sensors.

The synthesis of silica-based nanohybrid materials was exalted by this versatility, and new hybrid nanosynthons need to be developed and extended to other new organic functions. This is the aim of our work. We are interested in the synthesis and characterization of new silica-based nano-objects by the chemical modification of silica nanoparticules. In addition, the effect of pH on the stabilization of the initial colloidal solution is studied by using two silica sols, Ludox AS40 and TMA. Both are silica colloidal solutions of about 24 ± 2 nm particles; the first is alkaline (pH 9), whereas the later is acid-stabilized (pH 5). As dipyridine has proved to be a very good ligand in transition metal chemistry, the preparation of silica-based materials possessing a covalently bonded dipyridine functionality would be of a great interest. Structural properties such as a rigid chelating bidentate ligand and, furthermore, electronic properties with an intense $\pi \rightarrow \pi^*$ transition implicated in ligand-to-metal charge transfer transition in metal complexes make them a prime tool for the synthesis of new hybrid nanosynthons. In connection to our work on the functionalization of silica nanoparticles by metallic complexes, these materials would be useful in the potential applications cited above. Very few syntheses of pyridine-modified silicas have been published in the literature. Lin and co-workers have initially reported the synthesis of dialkylaminopyridine-functionalized mesoporous MCM-type silicas as efficient heterogeneous catalysts for catalytic nucleophilic reactions.[59] The chemical accessibility and reactivity of the organic functionalities were also preserved after heating for template removal, as demonstrated by these same authors, with the coordination properties of dipyridine MCM-41-type mesoporous silicas toward ruthenium complexes.[60] Csögor and co-workers investigated ζ-potential modification of silica nanoparticules by coupling isocyanatopropyl- or glycidoxypropylsilane with various diamines in order to obtain positively charged nanoparticules for DNA immobilization.[50] Herein, we report on a systematic investigation of the grafting reaction of two types of colloidal silica (AS40 and TMA) with 4-methyl-4′-(methylaminopropyltriethoxysilyl)-2,2′-dipyridine, **5**; 4-methyl-4′-(methylaminopropyldimethylethoxysilyl)-2,2′-dipyridine, **6**; ureidopropyltrimethoxysilane, **7**; and isocyanatopropyltrimethoxysilane, **8**, as silylating agents. Organically modified silica nanoparticules were synthesized via a grafting reaction in water or a 1:1 alcohol/water mixture (v/v) using various organosilane-to-silica ratios and characterized using solid-state NMR,

Scheme 2. Structure of the Nanohybrids

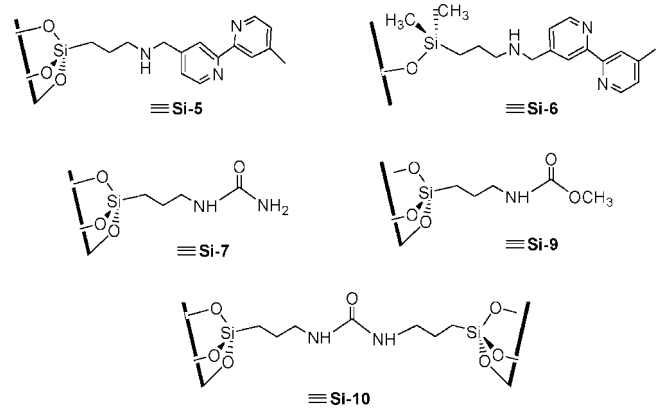

diffuse reflectance IR Fourier transform (DRIFT), N_2 adsorption, thermogravimetric and differential thermal analyses (TGA/DTA), and elemental analysis. scanning and transmission electron microscopies (SEM and TEM) were used to confirm the morphology and size of the nanoparticules. The aminomethyldipyridine functionality was chosen to represent common and stable metal-binding ligands; the ureido derivatives in addition to their filler properties for polymers[61] or adsorption properties[62,63] were used as spectroscopic probes for managing the grafting reaction. We have demonstrated that it is possible to efficiently functionalize silica nanoparticules, yielding materials with a homogeneous spatial distribution of organic groups, while fully preserving the chemical integrity of the organic functional groups, except for the isocyanato moiety, which brings two new organic functions on the silica surface, namely, 3-silylpropylurethan, **9**, when reacting in ethanol and *N*,*N*′-bis[3-silylpropyl]urea, **10**, as a dipodal functionality when reacting in water (Scheme 2).

2. Experimental Section

2.1. Materials. Ludox AS40 and TMA, obtained from Aldrich, were used as starting silica materials. They contain respectively 40 and 34 wt % SiO_2, with an average particle size of 24 nm. 4,4′-Dimethyl-2,2′-dipyridyl (99.5%) was obtained from Aldrich, selenium dioxide from Merck, 1,4-dioxane from SDS, sodium sulfite from Prolalo, and sodium borohydride (98%) from Acros.

The silylating agents 3-aminopropyltrimethoxysilane (APTMS, 97%); 3-aminopropyltriethoxysilane (APTES, 99%); 3-aminopro-

(59) Chen, H. T.; Huh, S.; Wiench, J. W.; Pruski, M.; Lin, V. S.-Y. *J. Am. Chem. Soc.* **2005**, *127*, 13305.
(60) Kumar, R.; Chen, H.-T.; Escoto, J. L. V.; Lin, V. S.-Y.; Pruski, M. *Chem. Mater.* **2006**, *18*, 4319.
(61) Domka, L.; Krysztafkiewicz, A.; Kozak, M. *Polym. Polym. Compos.* **2002**, *10*, 541.
(62) Santos, M. R. M. C; Airoldi, C. *J. Colloid Interface Sci.* **1996**, *183*, 416.
(63) Silva, C. R.; Airoldi, C.; Collins, E.; Collins, C. H. *J. Chromatogr., A* **2005**, *1087*, 29.
(64) Strouse, G. F.; Schoonover, J. R.; Duesing, R.; Boyde, S.; Jones, W. E.; Meyer, T. J. *Inorg. Chem.* **1995**, *34*, 473.
(65) ^{1}H NMR (δ ppm, $CDCl_3$): 2.47 (s, 3H, CH_3 (7), 7.20 (d, 1H, CH(5′), J = 6 Hz), 7.73 (d, 1H, CH(5), J = 6 Hz), 8.28 (s, 1H, CH(3′)), 8.58 (d, 1H, CH(6′), J = 6 Hz), 8.83 (s, 1H, CH(3)), 8.89 (d, 1H, CH(6), J = 6 Hz), 10.18 (s, 1H, CH(8)). ^{13}C{^{1}H} NMR (δ ppm, $CDCl_3$): 21.2 (1C, CH_3, C7), 120.6 (1C, CH, C3′), 121.3 (1C, CH, C5′), 122.1 (1C, CH, C5), 125.4 (1C, CH, C3), 142.6 (1C, C, C4), 148.4 (1C, C, C4′), 149.2 (1C, CH, C6′), 150.3 (1C, CH, C6), 154.7, 158.3 (2C, C, C2, 2′), 191.7 (1C, CH, C8). IR (KBr, cm^{-1}): 1708 ν(C=O), 1606, 1557 δ(dipyridine), 1460 δ(CH_3). AE found (calcd): C 71.89 (72.64), H 5.04 (5.37), N 13.50(14.12) %. UV (EtOH): 230.1 nm (ε = 12 071 L mol^{-1} cm^{-1}), 280.2 nm (ε = 5130 L mol^{-1} cm^{-1}), 318.4 nm (ε = 579 L mol^{-1} cm^{-1}). SM (DCI/NH_3): m/z = 199 $[M+H]^+$.

pyldimethylmethoxysilane (APDMMS, 97%); 3-ureidopropyltrimethoxysilane (97%), **7**; and 3-isocyanatopropyltrimethoxysilane (95%), **8**, were purchased from ABCR and used without purification. Chloroform, dichloromethane, methanol, and ethanol were purified by distillation in an inert atmosphere before use. 4′-Formyl-4-methyldipyridyl, **1**, was synthesized as previously described by Strouse et al.,[64] and characterization by elemental analysis (AE), infrared (IR), ultraviolet (UV), single molecule (SM), and ^{1}H and ^{13}C{^{1}H} spectroscopies are given in ref 65. All manipulations concerning the preparation of the silanes were performed in an inert atmosphere using the Schlenk tube technique. Aqueous solutions were prepared with ultrapure water (18.2 MΩ cm^{-1}) obtained from a Millipore milliQ water purification system.

2.2. Characterizations. Dipyridine silylating agents were characterized by infrared spectroscopy in the range 4000–400 cm^{-1} with a Bruker Vector 22 spectrophotometer. The spectrometer was calibrated with a standard polystyrene film. Solid samples were prepared as a KBr disk, whereas liquid samples were used pure. ^{1}H and ^{13}C {^{1}H} NMR spectra in $CDCl_3$ were measured using a Bruker Avance 300 (300.180 and 75.468 MHz for ^{1}H and ^{13}C, respectively). Chemical shifts (δ) are given in parts per million, relative to the solvent signal; signal multiplicity is noted as s = singlet, d = doublet, t = triplet, q = quadruplet, and m = multiplet. Coupling constants (J) are expressed in hertz. Mass spectra were recorded by chemical ionization (NH_3) or electronic impact using a Nermag R10-10 spectrometer or a TSQ 7000 Thermo-Quest Spectrometer. UV spectra were recorded using a Varian UV–visible Cary 1E spectrometer in the range 200–900 nm.

We have characterized chemically modified silica nanoparticles by infrared spectroscopy using the diffuse reflectance technique (Perkin-Elmer 1760 X with DTGS detector) and ^{29}Si and ^{13}C solid-state NMR (Bruker Avance 400 WB) using dipolar decoupling in combination with cross-polarization (CP) and magic angle spinning (MAS). The measurements were obtained in natural abundance at frequencies of 100.356 and 79.391 MHz for carbon and silicon, respectively. The amount of grafted organic material on each sample was determined by elemental analysis of C, H, and N performed on a Carlo Erba instrument (EA 1110). Simultaneous thermogravimetric (TG) and differential thermal (DT) analyses were carried out on a SETARAM TG-DTA 92 thermobalance using 20 mg of the sample; α-alumina was used as a reference. The heating rate was 3.8 °C/min. The temperature range was 20–1200 °C, and the analyses were done using a 1.5 L h^{-1} air flow.

TEM and SEM were used to determine the morphology and particle size. TEM analyses were done on a JEOL 2010 (200 kV). A drop of sol was diluted in ethanol. Then, a carbon-coated grid was dipped in the solution and allowed to dry at room temperature. SEM analyses were done on a JEOL JSM 6700 F. The nitrogen adsorption–desorption isotherms were determined at 77 K, using a volumetric method, with a Micromeritics ASAP 2010M. The isotherms were recorded in the 0.01−0.995 relative pressure range. Nitrogen of high purity (99.999%) was used. Samples were outgassed for 3 h at 80 °C under a vacuum before analysis. Some specific surface areas were also determined using a Micromeritics Flowsorb II 2300 instrument. In this case, the samples were previously outgassed for 3 h at 80 °C in a high-purity N_2 flow.

2.3. Synthesis. *2.3.1. Preparation of Dipyridine Derivatives.* 4-Methyl-4′-(iminopropylalkoxysilyl)-2,2′-dipyridine (**2**−**4**). 4′-Formyl-4-methyldipyridyl, **1**, (840 mg, 4.24 mmol) was reacted with appropriate silylating agents APTMS (0.763 mL, 4.24 mmol), APTES (0.999 mL, 4.24 mmol), or APDMMS (0.751 mL, 4.24 mmol) in chloroform (30 mL) with constant stirring for 3 h at room temperature. Removing the solvent in vacuo gave a colorless oil that was treated three times with chloroform to yield **2**−**4** quantitatively.

Comnpound **2**. IR ($CHCl_3$, cm^{-1}): 2947 $\nu_{as}(CH_3, CH_2)$, 2845 $\nu_s(CH_3, CH_2)$, 1650 ν(C=N), 1597, 1556 δ(dipyridine), 1465 $\delta(CH_3)$, 1383 $\delta(CH_2)$, 1251 ν (Si−C), 1088 ν(Si−O−C), 901 δ(Si−O), 726 $\delta(CH_3, CH_2)$. UV (EtOH): 235.1 nm (ε = 16 621 L mol^{-1} cm^{-1}), 281.2 nm (ε = 6407 L mol^{-1} cm^{-1}), 304.4 nm (ε = 4447 L mol^{-1} cm^{-1}). SM (DCI/NH_3): m/z = 360 [M + H]$^+$.

Compound **3**. ^{29}Si NMR (δ ppm, $CDCl_3$): −45.4 (s). IR (pure, cm^{-1}): 2970 $\nu_{as}(CH_3, CH_2)$, 2890 $\nu_s(CH_3, CH_2)$, 1649 ν(C=N), 1591, 1553 δ(dipyridine), 1455 $\delta(CH_3)$, 1389 $\delta(CH_2)$, 1252 ν(Si−C), 1076 ν(Si−O−C), 956 δ(Si−O), 757 $\delta(CH_3, CH_2)$. UV (CH_2Cl_2): 237.3 nm (ε = 22 390 L mol^{-1} cm^{-1}), 279.9 nm (ε = 8212 L mol^{-1} cm^{-1}), 304.4 nm (ε = 6044 L mol^{-1} cm^{-1}). SM (DCI/NH_3): m/z = 402 [M + H]$^+$.

Compound **4**. ^{29}Si NMR (δ ppm, $CDCl_3$): 19.6 (s). IR (pure, cm^{-1}): 2924 $\nu_{as}(CH_3, CH_2)$, 2854 $\nu_s(CH_3, CH_2)$, 1648 ν(C=N), 1593, 1553 δ(dipyridine), 1456 $\delta(CH_3)$, 1402 $\delta(CH_2)$, 1252 ν (Si−C), 1086 ν(Si−O−C), 955 δ(Si−O), 754 $\delta(CH_3, CH_2)$. UV (CH_2Cl_2): 237.3 nm (ε = 29 482 L mol^{-1} cm^{-1}), 280.2 nm (ε = 11 264 L mol^{-1} cm^{-1}), 302.4 nm (ε = 8154 L mol^{-1} cm^{-1}). SM (DCI/NH_3): m/z = 328 [M + H]$^+$.

4-Methyl-4′-(methylaminopropylalkoxysilyl)-2,2′-dipyridine (**5**, **6**). Appropriate iminomethyldipyridyl derivatives, **2** (359 mg, 1 mmol), **3** (401 mg, 1 mmol), and **4** (327 mg, 1 mmol), diluted in absolute ethanol (50 mL) were reacted with sodium borohydride (76 mg, 2 mmol) at room temperature for 18 h. Solvent was evaporated to give a gray powder. Excess borohydride was then hydrolyzed with water (30 mL); **5** and **6** were obtained by three extractions with dichloromethane (30 mL). The organic phase was allowed to dry on sodium sulfate for 3 h and then was filtrated, and solvent was removed in vacuo to yield **5** (87%) and **6** (82%). Methoxy groups of compounds **2** and **4** were all exchanged in ethoxy groups in this reaction giving triethoxysilane-substituted compounds **5** and **6**, respectively. Compound **5** is also obtained from derivative **3**.

Compound **5**. ^{29}Si NMR (δ ppm, $CDCl_3$): −45.3 (s). IR (pure, cm^{-1}): 3308 ν(NH), 2928 $\nu_{as}(CH_3, CH_2)$, 2884 $\nu_s(CH_3, CH_2)$, 1595, 1555 δ(dipyridine), 1456 δ(NH, CH_3), 1376 $\delta(CH_2)$, 1269 ν(Si−C), 1076 ν(Si−O−C), 958 δ(Si−O), 736 $\delta(CH_2,CH_3)$. UV (CH_2Cl_2): 242.5 nm (ε = 10 349 L mol^{-1} cm^{-1}), 283.8 nm (ε = 11 788 L mol^{-1} cm^{-1}). SM (DCI/NH_3): m/z = 403 [M]$^+$.

Compound **6**. ^{29}Si NMR (δ ppm, $CDCl_3$): 7.6 (s). IR (pure, cm^{-1}): 3306 ν(NH), 2960 $\nu_{as}(CH_3, CH_2)$, 2857 $\nu_s(CH_3, CH_2)$, 1597, 1556 δ(dipyridine), 1460 δ(NH, CH_3), 1377 $\delta(CH_2)$, 1252 ν(Si−C), 1071 ν(Si−O−C), 993 δ(Si−O), 735 $\delta(CH_3, CH_2)$. UV (EtOH): 240.0 nm (ε = 16 829 L mol^{-1} cm^{-1}), 282.9 nm (ε = 19 168 L mol^{-1} cm^{-1}). SM (DCI/NH_3): m/z = 344 [M + H]$^+$.

See the assigned ^{1}H and ^{13}C {^{1}H}NMR data for all compounds in the Supporting Information.

2.3.2. General Procedures for the Preparation of Silica-Based Nanohybrids. A total of 2.4 g of Ludox silica sol (7 g TMA sol; 6 g AS40 sol) was diluted with ultrapure water or alcohol. An ultrapure water−ethanol mixture (25:25 mL) was used for **5** and **6** and water or water–methanol for **7** and **8**. The homogeneous dispersion was mixed with 1.93–4.84 g (4.80–12.00 mmol) of **5** or 1.65–4.12 g (4.80–12.00 mmol) of **6**, 0.10–2.32 mL (0.48–12.00 mmol) of **7**, and 0.93–2.32 mL (4.80–12.00 mmol) of **8**. The solutions were left 72 h under stirring at 295 K. At the end of the reaction, the sample was centrifuged at 17 000 rpm for 5 min The clear supernatant was decanted from the solid deposit composed of the grafted particles. The obtained solid mass was washed with ethanol or methanol, dichloromethane, and diethyl ether and then dried in vacuo for 2 h. The liquid phase was dialyzed in pure water until the conductivity was equal to the pure water one. One part of the dialyzed liquid containing modified colloidal silica was dried

Scheme 3. Synthesis of Dipyridyl Derivatives 5 and 6

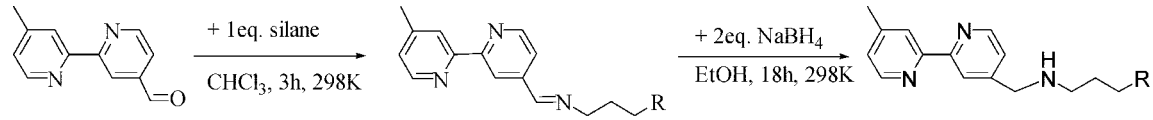

R = $Si(OMe)_3$ ***1***; $Si(OEt)_3$ ***2***; $Si(CH_3)_2(OMe)$ ***3*** R = $Si(OEt)_3$ ***4***; $Si(CH_3)_2(OEt)$ ***5***

in order to recuperate modified silica particles for solid state analysis. The resulting grafted silica particles were kept in a closed flask ready for further use. In order to check reproducibility, experiments were carried out in triplicate. Characterizations by DRIFT, CP MAS NMR, TGA, and nitrogen adsorption at 77 K are detailed for each of the silicated materials for an organic-to-silica ratio equal to 2 mmol g^{-1}. They are noted as ≡**ASi-X** or ≡**TSi-X**, with X corresponding to the organic molecule number, and A and T respectively refer to AS40 or TMA colloidal silicas.

≡**TSi-5**. τ = 0.87 mmol/g. AE found (calcd): C 14.86 (15.66), H 1.72 (1.57), N 3.65 (3.65) %. τ = 0.88 mmol/g by TGA. BET surface area (m^2/g): 43. DRIFT (cm^{-1}): 3285 ν(NH), 2928 $\nu_{as}(CH_3, CH_2)$, 2856 $\nu_s(CH_3, CH_2)$, 1596, 1554 δ(dipyridine), 1460 δ(NH, CH_3), 1377 $\delta(CH_2)$, 1207 ν(Si−C), 1114 ν(Si−O−Si), 949 δ(Si−O), 815 δ(Si−O). ^{29}Si CP MAS NMR (δ ppm): −59 (T^2), −68 (T^3), −101 (Q^3), −111 (Q^4). ^{13}C CP MAS NMR (δ ppm): 11.0 (C11), 20.8 (C7), 24.1 (C10), 52.5 (C8; C9), 122.0 (C3, 3′; C5, 5′), 148.8 (C6, 6′; C4, 4′), 155.8 (C2, 2′).

≡**ASi-6**. τ = 0.28 mmol/g. AE found (calcd): C 5.93 (5.04), H 0.92 (0.67), N 1.18 (1.18) %. τ = 0.33 mmol/g by TGA. BET surface area (m^2/g) 69. DRIFT (cm^{-1}): 3295 ν(NH), 2957 $\nu_{as}(CH_3, CH_2)$, 2840 $\nu_s(CH_3, CH_2)$, 1597, 1555 δ(dipyridine), 1461 δ(NH, CH_3), 1376 $\delta(CH_2)$, 1211 ν(Si−C), 1115 ν(Si−O−Si), 956 δ(Si−O), 802 δ(Si−O). ^{29}Si CP MAS NMR (δ ppm): +11 (M), −100 (Q^3), −110 (Q^4). ^{13}C CP MAS NMR (δ ppm): 0.4 (C12), 15.9 (C11), 21.0 (C7), 23.9 (C10), 52.8 (C8; C9), 120–124 (C3, 3′; C5, 5′), 149.0 (C6, 6′; C 4, 4′), 156.2 (C2, 2′).

≡**ASi-7**. τ = 0.74 mmol/g. AE found (calcd): C 2.71 (3.55), H 0.79 (0.67), N 2.07 (2.07) %. τ = 0.88 mmol/g by TGA. BET surface area (m^2/g): 110. DRIFT (cm^{-1}): 3340, 3200 ν(NH), 2930 $\nu_{as}(CH_3, CH_2)$, 2878 $\nu_s(CH_3, CH_2)$, 1651 ν(CO), 1610 $\delta(NH_2)$, 1560 δ(CNH), 1443 δ(NH, CH_3), 1347 $\delta(CH_2)$, 1203 ν(Si−C), 1114 ν(Si−O−Si), 952 δ(Si−O), 803 δ(Si−O). ^{29}Si CP MAS NMR (δ ppm): −58 (T^2), −67 (T^3), −101 (Q^3), −110 (Q^4). ^{13}C CP MAS NMR (δ ppm): 10.5 (C11), 24.0 (C10), 43.3 (C9), 161.1 (C8).

≡**TSi-9**. τ = 1.26 mmol/g. AE found (calcd): C 6.09 (7.56), H 1.28 (1.26), N 1.76 (1.76) %. τ = 1.06 mmol/g by TGA. BET surface area (m^2/g): 97. DRIFT (cm^{-1}): 3319 ν(NH), 2940 $\nu_{as}(CH_3, CH_2)$, 2880 $\nu_s(CH_3, CH_2)$, 1700 ν(CO), 1560 δ(NH), 1443 δ(NH, CH_3), 1347 $\delta(CH_2)$, 1201 ν(Si−C), 1121 ν(Si−O−Si), 930 δ(Si−O), 802 δ(Si−O). ^{29}Si CP MAS NMR (δ ppm): −58 (T^2), −67 (T^3), −101 (Q^3), −110 (Q^4). ^{13}C CP MAS NMR (δ ppm): 10.0 (C11), 23.8 (C10), 43.3 (C9), 52.0 (C15), 158.4 (C8).

≡**TSi-10**. τ = 0.69 mmol /g. AE found (calcd): C 5.71 (5.80), H 1.32 (0.97), N 1.93 (1.93) %. τ = 0.73 mmol /g TGA. BET surface area (m^2/g): 116. DRIFT (cm^{-1}): 3318 ν(NH), 2933 $\nu_{as}(CH_3, CH_2)$, 2878 $\nu_s(CH_3, CH_2)$, 1641 ν(CO), 1560 δ(CNH), 1443 δ(NH, CH_3), 1340 $\delta(CH_2)$, 1205 ν(Si−C), 1122 ν(Si−O−Si), 920 δ(Si−O), 801 δ(Si−O). ^{29}Si CP MAS NMR (δ ppm): −57 (T^2), −67 (T^3), −101 (Q^3), −110 (Q^4). ^{13}C CP MAS NMR (δ ppm): 10.1 (C11), 24.1 (C10), 42.5 (C9), 160.2 (C8).

3. Results and Discussion

3.1. Synthesis of Organosilanes 4-Methyl-4′-(methylaminopropyltriethoxysilyl)-2,2′-dipyridine (5) **and 4-Methyl-4′-(methylaminopropyldimethylethoxysilyl)-2,2′-dipyridine** (6)**.** Organosilanes were synthesized in good yields via a procedure described in the Experimental Section. We synthesized both triethoxysilane and dimethylethoxysilane derivatives (**5** and **6**) because of the reactivity expected for the latter. Silane coupling agents with three alkoxy groups as usual starting points for substrate modification tend to deposit as a polymeric film, effecting the total coverage and maximizing the presentation of organic functionality. Intrinsic limitations in the utilization of a polylayer deposition are significant for nanoparticules or nanocomposites where the interphase dimensions generated by polylayer deposition may approach those of the substrate. So, monoalkoxysilanes provide an interesting alternative for nanofeatured substrates, since, with only one alkoxy function, grafting is limited to the monolayer. The experimental conditions of the grafting reaction of triethoxysilane **5** have to be controlled to minimize polymerization, as usually expected with these precursors. Moreover, for the further reactivity expected for these nanohybrids, that is, application in a biological medium or complexation reactions, amines are well-known to be more stable to pH change than amides or imines. So, we focused on the reduction reaction in order to obtain stable amino compounds **5** and **6**. They were synthesized in two steps (Scheme 3), first by transformation of the aldehyde function in **1** to the imine one in **2**−**4** quantitatively. Then, the reduction by sodium borohydride in ethanol gave the aminomethyldipyridine derivatives, **5** and **6**, with 87 and 82% global yields.

These reactions were monitored by ^{1}H NMR spectroscopy where we controlled the hydrogen atom of the aldehyde function at 10.2 ppm, which was replaced by the imine signals at 8.71 (**2**), 8.52 (**3**), and 8.63 ppm (**4**) in the first step, followed by a transformation in the methylene signal of the methylamino group at 3.89 and 3.78 for **5** and **6**, respectively. While signals corresponding to the dipyridine backbone were relatively unchanged, the three signals corresponding to the propyl chain, which appeared in the ranges 0.61–0.67, 1.49–1.79, and 3.61–3.73 ppm for imine compounds **2**−**4**, were more sensitive to the imine−amine transformation. This is especially true for the methylene hydrogen atoms in the α position of the amine nitrogen atom, which are upfield-shifted at 2.65 and 2.55 ppm respectively for **5** and **6**. Completion of the reduction was also confirmed with ^{13}C{^{1}H} NMR spectroscopy, in agreement with the significant upfield shift of carbon atoms from 160.0 to 158.9 ppm for imine compounds to 53.4 and 52.6 ppm for **5** and **6**,

Table 1. Grafting Amounts for Each Nanohybrid Obtained by Elementary Analysis

experiment set	silica pH	solvent	organosilane /silica (mmol/g)	τ, grafted amount (mmol/g) ≡Si-5	≡Si-6	≡Si-7	≡Si-9	≡Si-10
1	AS40 9	H_2O/alcohol 1:1	2	1.24	0.28	0.74	1.28	
2			5	1.81	0.61	1.18		
3		H_2O	2			0.50		0.65
4			5			1.34		0.61
5	TMA 5	H_2O/alcohol 1:1	2	0.87	0.77	0.63	1.26	
6			5	1.76	0.41	1.91		
7		H_2O	2			0.91		0.69
8			5			1.84		0.65
9		Acetate buffer	2	0.29		0.31		0.35
10			5	0.31		1.63		0.43

respectively. During the later reaction, which proceeds in ethanol and requires hydrolysis of the hydride excess, we observed exchange between methoxy and ethoxy substituents of the silane group via a transesterification reaction. This is confirmed by both ^1H and $^{13}C\{^1H\}$ NMR spectra. This reactivity, well-known in silane chemistry,[66,67] explains why the 4-methyl-4′-(methylaminopropyltriethoxysilyl)-2,2′-dipyridine, **5**, was isolated from initial compounds **2** and **3** while monoethoxyderivative **6** was isolated from monomethoxy precursor **4**. Chemical transformations of organic functions from aldehyde into amine were also clearly apparent in the IR spectra, and significant vibrations are available in the Supporting Information. Classical propyl chain stretching vibrations appeared between 2924 and 2970 (ν_{as}) and 2845 and 2890(ν_s) with bending vibrations at 1455–1465 and 1376–1402 cm^{-1}. NH stretching and bending are observed for compounds **5** and **6** at 3308 and 3306 cm^{-1} respectively and 1456 and 1460 cm^{-1} respectively. The bending NH band overlapped the CH_3 bending vibration. The spectra of all compounds also exhibit bending deformations of the dipyridyl moiety as two medium and sharp bands at 1591–1597 and 1553–1556 cm^{-1}. An alkoxysilyl function with characteristic bands at 1071–1088 cm^{-1} (stretching Si−O−C) and 901–993 cm^{-1} (bending Si−O) confirmed that target molecules were indeed synthesized. Spectra of **4** and **6** differ from the others by the strong ν(Si−C) vibration at 1252 cm^{-1}. The molecular structures of iminomethyl- (**2**−**4**) and aminomethyl-dipyridine (**5** and **6**) were definitively ascertained by mass spectrometry since DCI/NH_3 mass spectra show the molecular peaks at $m/z = 360$, 402, 328, 403, and 344 for compounds **2**−**6**, respectively, for $[M+H]^+$ or $[M]^+$ species.

3.2. Synthesis of Silica-Based Nanohybrids. We have investigated the grafting reaction of four organosilanes with aqueous colloidal silicas in order to demonstrate that it would be possible to obtain, under mild conditions, tailored silica surfaces, with a homogeneous repartition of various organic functions on individual particles of about 30 nm diameter. A lot of parameters were evaluated such as run time, temperature, and solvent, but three were found to be critical, that is, the initial pH of the colloidal solution, organosilane-to-silica ratio, and chemical properties of the organosilane. Reflux heating or only 24 h of a stirring reaction at 295 K gave nonhomogeneous nanohybrids. So, reactions were realized, by stirring for 3 days at 295 K, a water or water/alcohol mixture of organosilane with AS40 or TMA Ludox silica. In addition, for TMA silica, an acetate buffer was used to maintain acid conditions during the grafting reaction. Grafting ratios, τ, in millimoles of organosilane per gram of silica materials are computed from the nitrogen content obtained by elemental analysis. They are confirmed by thermogravimetric data. The results of reactions realized under these three conditions are reported in Table 1, and a simplified representation of the five corresponding nanohybrids is given in Scheme 2.

Assuming that the average surface occupied by one organic molecule is 0.25 nm^2 (as proposed by Dulcey and coworkers[68]), and taking a specific surface area of 140 $m^2\ g^{-1}$ for silica nanoparticules (TMA or AS40), the maximum amount expected for a 100% monolayered coverage would be about 1 mmol of organosilane per gram of silica materials. TGA gave 5.0 and 5.7 silanol sites nm^{-2} respectively for TMA and AS40 silica, which is in agreement with the commonly admitted 3–5 silanol sites nm^{-2} available for the condensation of organosilane molecules on the silica surface.[1] The maximum theoretical grafted amount is not so easily accessible, even in organic solvent, because of the hindrance of the organosilane and its homocondensation reaction, which is always possible. Scheme 4 shows first concurrent reactions which usually occur in a water/alcohol medium such as (i) the hydrolysis of organosilane; (ii) oligomerization from hydrolyzed species; (iii) a grafting reaction described as hydrolyzed or homocondensated organosilane condensation on a silanol site of the silica surface; a complete initial hydrolysis of organosilane was excluded on the basis of the lowest reactivity of alkyltrialkoxysilane and because the condensation reaction always begins before hydrolysis is complete;[67,69] so, we have studied the reaction in an excess of organosilane in order to demonstrate different functionalizations available on the silica surface; (iv) organosilane oligomer grafting; or (v) organosilane monolayer grafting. Because surface properties were of importance for further stabilization in suspension and chemical functionalization, both nanohybrid types are interesting for chemistry and applications targeted (Scheme 1).

(66) Birkofer, L.; Stuhl, O. General Synthetic Pathways to Organosilicon Compounds. In *The chemistry of organic silicon compounds*; Patai, S., Rappoport, Z., Eds.; Wiley and Sons: New York, 1989; p 655.
(67) Brinker, C. J.; Scherer, G. W. *Sol-Gel Science, The Physics and Chemistry of Sol-Gel Processing*; Academic Press: San Diego, CA, 1990.
(68) Dulcey, C. S., Jr.; Chen, M.-S.; McElvany, S. W.; O'Ferrall, C. E.; Benezra, V. I.; Calvert, J. M. *Langmuir* **1996**, *12*, 1638.
(69) Iler, R. K. *The chemistry of silica*; Wiley: New York, 1979.

Scheme 4. A Few Concurrent Reactions Occurring in Solution and on the Silica Surface Affording Two Types of Functionnalization: Organosilane Oligomer Grafted Nanoparticles (*iv*) or Organosilane Monolayer Grafted Nanoparticles (*v*)

(i) Hydrolysis

$$R'Si(OR)_3 + H_2O \rightleftharpoons R'Si(OR)_2(OH) + ROH$$

$$R'(RO)_2Si\text{-}O\text{-}Si(OR)_2R' + H_2O \rightleftharpoons R'(RO)_2Si\text{-}O\text{-}Si(OH)(OR)R' + ROH$$

(ii) Oligomerization reactions

$$R'Si(OR)_3 + (HO)Si(OR)_2R' \rightleftharpoons R'(OR)_2Si\text{-}O\text{-}Si(OR)_2R' + ROH$$

$$R'Si(OR)_3 + R'(RO)_2Si\text{-}O\text{-}Si(OH)(OR)R' \rightleftharpoons R'(RO)_2Si\text{-}O\text{-}SiR'(OR)\text{-}O\text{-}SiR'(OR)_2 + ROH$$

linear trimer

$$R'(RO)_2Si\text{-}O\text{-}Si(OH)(OR)R' + R'Si(OR)_2(OH) \rightleftharpoons R'(RO)\overbrace{Si\text{-}O\text{-}SiR'(OR)\text{-}O\text{-}SiR'(OR)\text{-}O}^{\text{cyclic trimer}} + 2ROH$$

$$2\,R'Si(OR)_2(OH) \rightleftharpoons R'(OR)_2Si\text{-}O\text{-}Si(OR)_2R' + H_2O$$

$$R'(RO)_2Si\text{-}O\text{-}Si(OH)(OR)R' + R'Si(OR)_2(OH) \rightleftharpoons R'(RO)_2Si\text{-}O\text{-}SiR'(OR)\text{-}O\text{-}SiR'(OR)_2 + H_2O$$

linear trimer

(iii) Grafting reaction on silica surface

$$R'Si(OR)_3 + HO\mathbf{SiO_2} \rightleftharpoons R'(RO)_2Si\text{-}O\mathbf{SiO_2} + ROH$$

$$R'(RO)\overbrace{Si\text{-}O\text{-}SiR'(OR)\text{-}O\text{-}SiR'(OR)\text{-}O} + HO\text{-}\mathbf{SiO_2} \rightleftharpoons \overbrace{O\text{-}R'(RO)Si\text{-}O\text{-}SiR'(OR)\text{-}OSiR'\text{-}O}\mathbf{SiO_2} + ROH$$

$$R'Si(OR)_2(OH) + HO\mathbf{SiO_2} \rightleftharpoons R'(RO)_2Si\text{-}O\mathbf{SiO_2} + H_2O$$

$$R'(RO)_2Si\text{-}O\text{-}Si(OR)_2R' + HO\mathbf{SiO_2} \rightleftharpoons R'(RO)_2Si\text{-}O\text{-}SiR'(OR)\text{-}O\mathbf{SiO_2} + ROH$$

(iv)

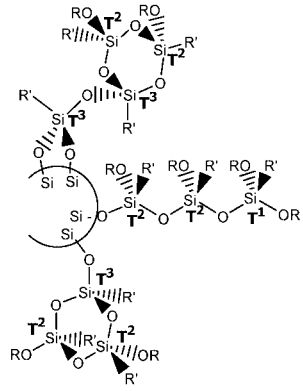

(v)

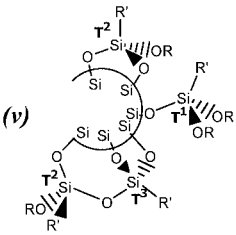

with R = Me, Et R' = alkyl group **SiO_2** represents silica framework

In screening experiments, commercial organosilane precursors, $(MeO)_3Si(CH_2)_3NHCONH_2$, **7**, and $(MeO)_3Si(CH_2)_3NCO$, **8**, were first introduced in gradual concentrations from 0.2 to 5 mmol g^{-1} of silica, but two ratios would be particularly interesting, giving structurally different nanohybrids (Scheme 4, iv and v). This is pointed out by the results obtained for organosilane with silica ratios equal to 2 and 5 mmol g^{-1}, which are reported in Table 1 for all organosilanes used in this work. Under our experimental conditions, the grafting reaction of organoalkoxysilane was faster than the homocondensation process, giving the chemically modified silica expected even after 3 days of reaction in water under both pH conditions. Purification was conducted by ultracentrifugation, giving a solid and a supernatant. The solid was successively washed, vortexed, and centrifuged, whereas the first supernatant was dialyzed. These treatments allowed the separation of grafted silicas from organosilane oligomers. Efficiency of the post treatments was demonstrated by the relatively low amounts (0.31–1.91 mmol g^{-1}) obtained when organosilane was in 5-fold excess. Results correspond to twice an excess of the organosilane yield, in most cases, a properly grafted organosilane monolayer on nanoparticles as characterized further in this paper, so these values allowed comparison.

The effect of the initial pH was evaluated using two Ludox silicas. So, we were able to compare first the initial pH effect and then the influence of steady acidic conditions when an acetate buffer is added to the mixture. In acidic conditions, because of the low homocondensation rate, the grafting reaction would be favorable, as observed by Posthumus and co-workers[32] and Francis and co-workers,[70] with metacryloxypropyltrimethoxysilane and glycidoxypropyltrimethoxysilane, respectively. We decided also to introduce alcohols known to be convenient solvents for such a reaction in order to increase organosilane solubility, minimize its hydrolysis, and therefore favor the grafting reaction.[1,67]

Isocyanato derivatives, **8**, as common precursors for urethans and ureas allow for the grafting of two new organic groups on the silica surface. In a water/methanol medium, isocyanate **8** reacts quantitatively with methanol to give silicated urethan ≡**Si-9**, whereas in an aqueous medium, **8** was hydrolyzed via

(70) Chu, L.; Daniels, M. W.; Francis, L. F. *Chem. Mater.* **1997**, *9*, 2577.

Scheme 5. Synthesis of Urethan ≡Si-9 and N,N′-urea ≡Si-10 Functionalized Silica Nanoparticles

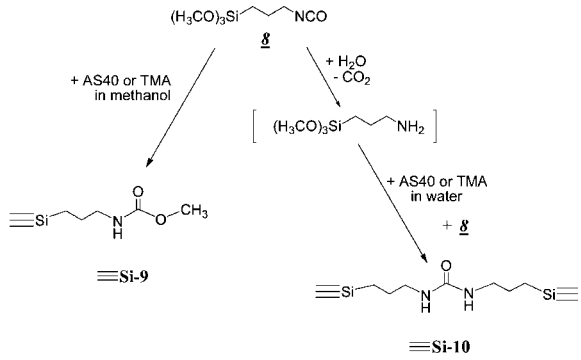

transient *N*-carbamic acid in primary amine, which reacts immediately with the excess of reactant to give silicated *N*,*N*′-disubstituted urea ≡**Si-10**. These reactions, according to Scheme 5, well-known in organic chemistry but never reported in silica surface chemistry, add two new synthons for our studies with interesting spectroscopic signatures.

Assuming two nitrogen atoms by a *N*,*N*′-disubstituted urea molecule, similar amounts of nitrogen contents were obtained for each grafted material under both solvent and pH conditions (experiment sets 1 and 5 for ≡**Si-9** versus experiment sets 3 and 7 for ≡**Si-10**), indicating for **8** no initial pH effect, neither on the grafting reaction nor on urea or urethan formation.

We observed a great inhibiting effect by the acid medium, comparing grafting ratios of 0.91 and 0.69 mmol g^{-1} respectively for ≡**Si-7** and ≡**Si-10** toward 0.31 and 0.35 mmol g^{-1} obtained when the pH was controlled by the addition of an acetate buffer (experiments 7 and 9). Very low grafted amounts demonstrated that, under steady acid conditions, because condensation is slow, the hydrolysis of organosilanes becomes limited, decreasing the yield of the grafting reaction.

With ureidopropylsilane, **7**, grafting ratios are rather better in methanol/water (experiment set 1) than in basic aqueous solution (experiment set 3), whereas it is the reverse in an acidic medium (experiment sets 5 and 7). A large range of grafting ratios (0.31–0.91 mmol g^{-1}) was obtained when solvent or pH conditions were modified, leading to various functionalized nanohybrids. The best grafting ratio is 0.91 mmol g^{-1}, obtained for ≡**Si-7** in experiment set 7.

Grafting reactions of dipyridylsilanes were done in a 1:1 mixture (v/v) of water and ethanol for the reasons explained above. Surprisingly, similar grafting ratios were obtained for both dipyridylsilanes **5** and **6** on TMA silica (experiment set 5), indicating monolayered coverage of the silica nanoparticles by both dipyridylsilanes with 0.87 and 0.77 mmol g^{-1} for ≡**Si-5** and ≡**Si-6**, respectively. Dimethylethoxysilane, **6**, because of the hindrance of the two methyl substituants on the silicon atom, gives a slightly lower grafting ratio. However, its functionalization is representative of the organosilane monolayer grafted nanoparticules. This is in agreement with the lower hydrolysis rate known for dimethylethoxysilane compared to that for trialkoxysilanes, together with a steric effect which favors grafting on isolated silanols toward homocondensation, increasing the grafting ratio.

In a basic medium (experiment set 1), homocondensation among hydrolysis species is the major reaction, giving a very low grafting ratio for ≡**Si-6** according to its specificity as a monoethoxysilane derivative; so oligomers are not able to condense on silanol sites. This is what happens with organosilane **5** when a value higher than 1 is reached for ≡**Si-5**, revealing an organosilane oligomer grafting on silica nanoparticules, as described in Scheme 4 (part iv). No explanation was found for the lowest grafting ratio obtained in a large excess of reactant **6** (experiment 6), unless, in this case, a high concentration favors the homocondensation of **6**, which stops the grafting reaction.

These results emphasized the chemical specificity of each organosilane molecule toward the expected reactivity on silicas. In all cases, high grafting ratios were obtained. Maximum amounts were reached for monolayered grafting, in particular, conditions such as TMA in water with 0.91 mmol g^{-1} for ≡**Si-7** and TMA in 1:1 water/ethanol with 0.87 and 0.77 mmol g^{-1} for ≡**Si-5** and ≡**Si-6**. Moreover, dimethylethoxysilane derivative **6** does not show a negative steric effect because of the presence of the two methyl groups on the silicon atom, which slightly bends organosilane on the silica surface. Finally, these experiments validated the preparation of homogeneous nanohybrids under mild conditions, in a large range of pHs, and with variable grafting ratios. In order to characterize the quality and the nature of the grafting, we have done an extended investigation of the grafted nanoparticules.

3.3. Characterization of the Particles' Compositions by TGA and DTA and DRIFT and CP MAS NMR Spectroscopies and Characterization of the Particles' Sizes and Morphologies by BET, SEM, and TEM Microscopies. Each compound family exhibits a specific behavior in thermal decomposition. In all samples, the first weight loss of 1.2–3.5%, in the temperature range 70−150 °C, can be ascribed to water desorption as an endothermic process. Further heating shows, for both dipyridine grafted materials ≡**Si-5** and ≡**Si-6**, three additional weight losses, as an exothermic process, at 200, 370, and 450 °C, the latter being the major. For ureas and urethane grafted materials ≡**Si-7**, ≡**Si-9**, and ≡**Si-10**, four weight losses were systematically observed at 280 (main), 350, 380, and 500 °C. As indicated in Table 2, weight losses resulting from organic moiety decomposition are in good agreement with the organic contents of materials calculated from nitrogen percentages obtained by elementary analysis. DRIFT analysis is a powerful tool, as it shows an unambiguous signature of each organic fragment (Supporting Information). As expected for ≡**Si-5** and ≡**Si-6**, two dipyridine ring vibrations are observed as sharp and intense bands at 1596, 1554, 1597, and 1555 cm^{-1}, respectively, in agreement with those of the free ligands. N-propylurea, propylurethan, and N,N′-bis(propyl) urea functional groups are easily identified according to different signatures of the amide vibrations in the range 1560–1700 cm^{-1}. N-urea in ≡**Si-7** exhibits two bending bands corresponding to −NHCO− and $-CONH_2$ vibrations at 1560 and 1610 cm^{-1} in addition to the CO stretching at 1651 cm^{-1}. Urethan and N,N′-urea in ≡**Si-9** and ≡**Si-10** give only two characteristic bands in the same range

Table 2. Physical Properties of the Silicated Nanohybrids[a]

	exp. set	S_{BET} ($m^2\ g^{-1}$)	C	τ in mmol g^{-1} EA	TGA
TMA		140	97	–	–
AS40		138	100	–	–
≡Si-5	5	43	37	0.87	0.90
≡Si-5	6	5		1.76	1.67
≡Si-6	1	69		0.28	0.33
≡Si-6	5	27	38	0.77	0.76
≡Si-7		128	66	0.33	
≡Si-7	1	108	67	0.74	0.88
≡Si-7	7	94		0.91	
≡Si-7	2	70	68	1.18	1.35
≡Si-7	10	59		1.63	
≡Si-7	6	37		1.91	
≡Si-7		<2		4.42	4.24
≡Si-9	5	97	67	1.26	1.06
≡Si-10	3	110		0.65	0.73

[a] Grafting ratio obtained by elemental (EA) and thermogravimetric (TGA) analyses.

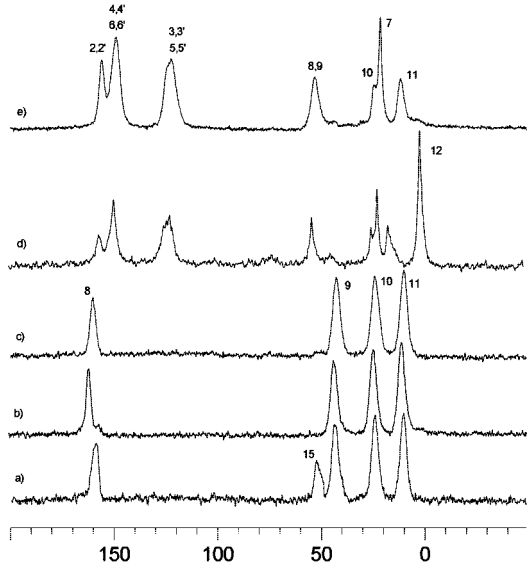

Figure 1. ^{13}C CP MAS NMR spectra of ≡**Si-9** (a), ≡**Si-7** (b), ≡**Si-10** (c), ≡**Si-6** (d), and ≡**Si-5** (e).

involving NHCO and CO vibrations at 1560 and 1700 cm^{-1} for urethane and 1560 and 1641 cm^{-1} for N,N′-substituted urea. Moreover, for all compounds, a pure NH stretching vibration is observed in the range 3200–3340 cm^{-1} together with bands at 2928–2957 $\nu_{as}(CH_3, CH_2)$ and 2840–2880 cm^{-1} $\nu_s(CH_3, CH_2)$ corresponding to the stretching vibrations of the propyl chain. A free silanol vibration observed at 3744 cm^{-1} in the spectra of pure silica has disappeared in all of the grafted materials, indicating the formation of the siloxane bond between organosilane and the silica surface via its reactive silanol sites. Moreover, the two characteristic Si−O−Si bands at 1179 and 1102 cm^{-1} in the pure silica spectrum were disturbed. There is a slight shift and broadening of the ν(Si−O−Si) stretching vibration in the range 1114–1122 cm^{-1} and the appearance of a strong ν(Si−C) vibration as a shoulder in the range 1201–1211 cm^{-1}.

The integrity of the organic functions is confirmed by ^{13}C CP MAS NMR spectroscopy. Assignments are reported in Figure 1 according to the carbon atom numbering illustrated in Scheme 6. We can identify all carbon resonances expected for each nanohybrid in agreement with those of the free organic molecules. No difference was observed between

Scheme 6. Numbering of the Carbon Atoms in 6 and ≡Si-9

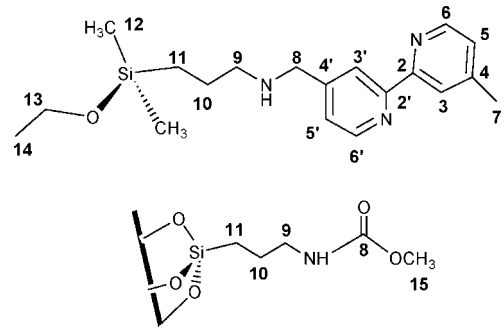

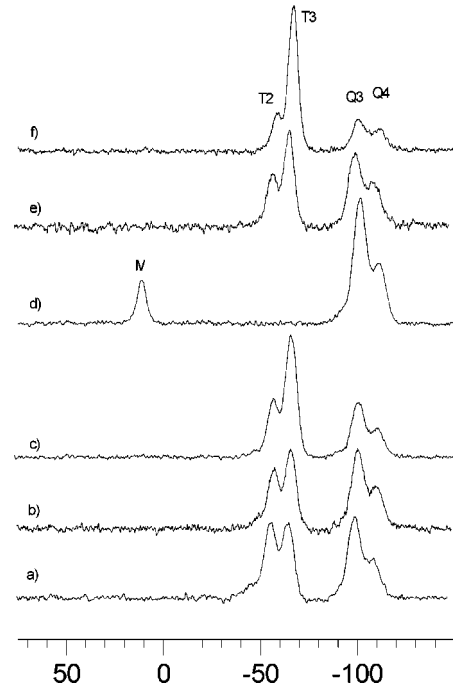

Figure 2. ^{29}Si CP MAS NMR spectra of ≡**Si-9** (a), ≡**Si-10** (b), ≡**Si-7** (c), ≡**Si-6** at 0.77 mmol g^{-1} (d), ≡**Si-5** at 0.87 mmol g^{-1} (e), and ≡**Si-5** at 1.76 mmol g^{-1} (f).

samples containing an oligomer or monomer grafted on silica. Resonances at 18 and 58 ppm of carbon atoms of the ethoxy group have never been observed in agreement with the aqueous conditions of grafting reactions.

This result is emphasized by ^{29}Si CP MAS NMR data (Figure 2), since the silicon atom of dipyridylsilane **6** appears at +11 ppm in ≡**Si-6** (Figure 1d) as expected for M-type grafted silicon atoms, whereas, in all other spectra, peaks at −58 and −68 are assigned to silicon atoms of hydrolyzed bidentate (T^2) or tridentate (T^3) silane, as usually reported in the literature for trialkoxysilane.[71,72] A signal at −53 ppm corresponding to T^1-type silicon atom types has never been observed in any samples using trialkoxysilane derivatives, even when **8** gives ≡**Si-10** in water. This is in agreement with the systematic absence of a linear oligomer grafted on the silica surface. This implies that dipodal silane in ≡**Si-10** reacts always with its two functions to form at least two siloxane bonds in agreement with the two peaks of equal intensity for T^2- and T^3-type silicon atoms shown

(71) Noll, W. *Chemie und Technologie der Silicone*, 2nd ed.; Verlag Chemie GMBH: Weinheim, Germany, 1968.
(72) Caravajal, G. S.; Leyden, D. E.; Quinting, G. R.; Maciel, G. E. *Anal. Chem.* **1988**, *60*, 1776.

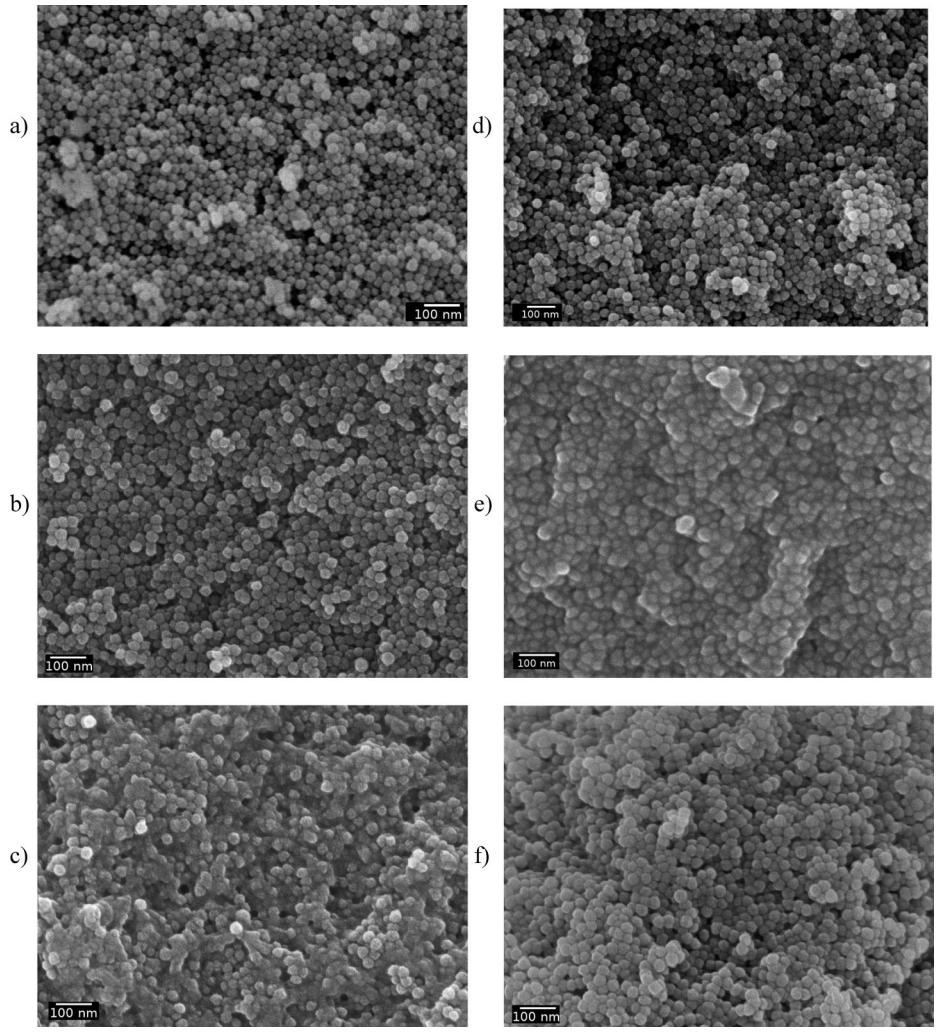

Figure 3. SEM micrographs of pure AS40 silica (a), ≡**Si-7** $\tau = 1.63$ mmol g^{-1} (b), ≡**Si-7** $\tau = 4.42$ mmol g^{-1}(c), ≡**Si-5** $\tau = 0.29$ mmol g^{-1} (d), ≡**Si-5** $\tau = 1.76$ mmol g^{-1} (e), and ≡**Si-6** $\tau = 0.28$ mmol g^{-1} (f).

in its spectra (Figure 2b). Unreacted Q^3 and Q^4 sites are detected at −101 and −110 ppm, confirming the presence of a silica matrix in all of the samples. Because of the nanometric size of the particles, the Q^3 signal is always more intense than the Q^4 siloxane signal.

The morphologies and sizes of the nanohybrids were examined using SEM and TEM. For all samples, characterized by a low grafting ratio (<1), the grafted silica surface looks like the surface of pure silica particles (Figure 3a,b,d,f). No difference in morphology was observed according to the chemical structure of the organosilane. TEM micrographs (Figure 4) show that monodispersity of nanosized particles was conserved after grafting. Only a slight increase in their average diameter is noticed: 25 ± 2 nm for all nanohybrids. Close observation reveals that the grafted silica surface is homogeneous. This is important for further investigation on silica nanohybrids.

Even if CP MAS NMR data are not quantitative to directly determine the grafting ratio, it is still possible to compare the relative intensity of T^2 and T^3 signals toward the Q^3 and Q^4 of samples exhibiting same organic function realized under the same experimental conditions.[56] More interesting is the evolution of silicon NMR spectra when the grafting ratio of ≡**Si-7** is increased from 0.50, 0.80, 1.18, and 1.63 to 4.42 mmol/g as illustrated in Figure 5. In order to promote the polymerization reaction the last sample was obtained by two ways. First, silica nanoparticules were reacted with a 7-fold excess of ureidopropylsilane **7**. In a second reaction, organosilane was first hydrolyzed in aqueous solution for 8 h before the addition of colloidal silica. The same post treatment as reported above was applied for purification before analysis. In this case, the T^3 signal is essentially observed in the ^{29}Si CP MAS NMR spectrum (Figure 5e) together with a few T^2 silicon atom types, indicating a large oligomerization reaction on the silica surface, for which the signature is negligible.

The evolution of morphology of the grafted materials along with the organic content is illustrated for ≡**Si-7** with Figures 3 and 5. We can see that individual particles are saved up to 1.63 mmol g^{-1}(Figure 5b), while they are glued in oligomerized organosilane (Figure 5c) when organosilane is in large excess. A similar comparison can be done between SEM micrographs of ≡**Si-5** (Figure 3d,e) and ^{29}Si CP MAS NMR data (Figure 2e,f). When the grafting ratio value reaches 1.76 mmol g^{-1} for dipyridylnanohybrid ≡**Si-5**, particles are glued in oligomerized organosilane as indicated by very small Q^4 and Q^3 signals together with the decrease in surface area values (Table 2). These results are demonstrative, for dipyridylsilane, of both functionalizations: orga-

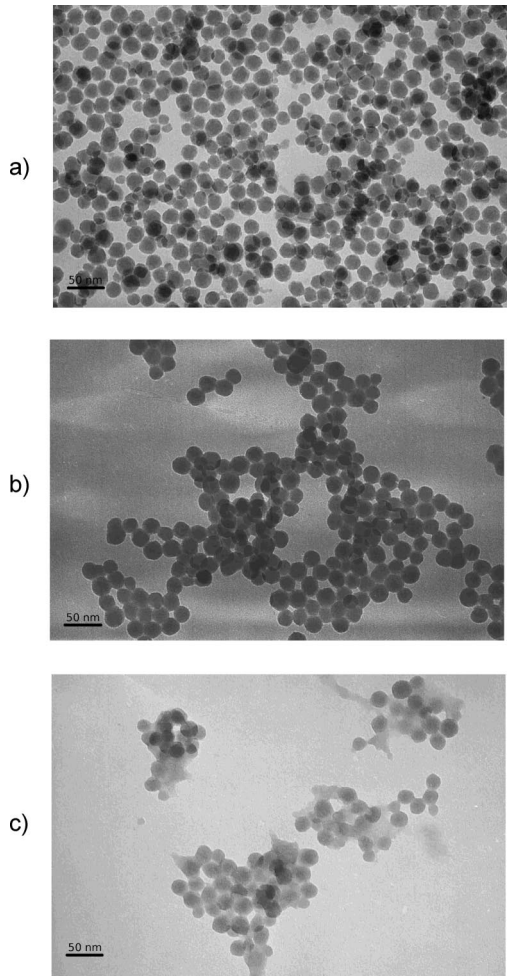

Figure 4. TEM micrographs of ≡**Si-5** with $\tau = 0.29$ mmol g^{-1} (a) and ≡**Si-7** with $\tau = 0.80$ mmol g^{-1} (b) and $\tau = 4.42$ mmol g^{-1} (c).

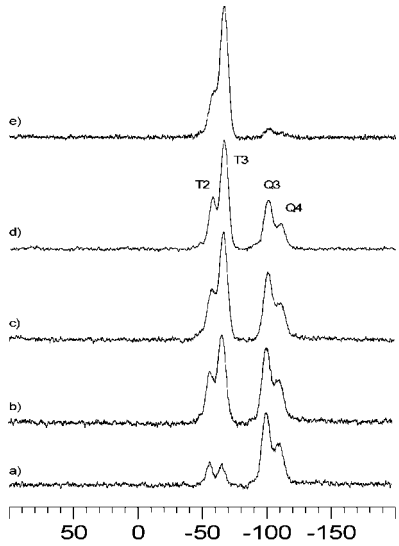

Figure 5. ^{29}Si CP MAS NMR spectra of ≡**Si-7** for increasing grafting amounts τ =0.50 (a), 0.80 (b), 1.18 (c), 1.63 (d), and 4.42 mmol g^{-1} (e).

nosilane oligomer grafted nanoparticules in the case of experiment set 6 (grafting ratio of 1.76 mmol.g^{-1}) and

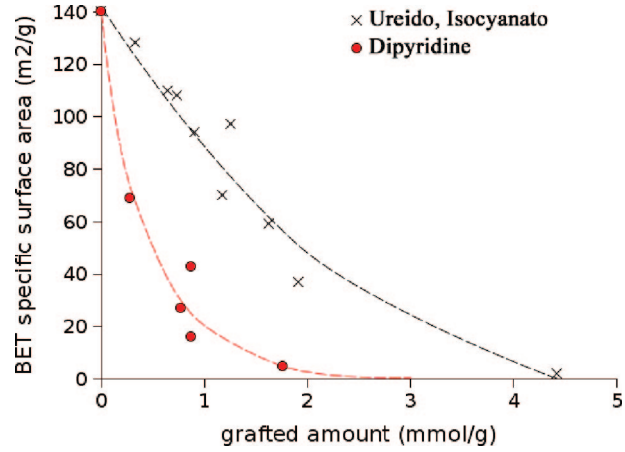

Figure 6. Plot of grafted amount vs BET area for bipyridine (●) and urea (x) derivatives.

organosilane monolayer grafted nanoparticules in experiment set 9 (grafting ratio of 0.29 mmol g^{-1}).

This is in agreement with the specific surface area, computed from the N_2 adsorption isotherms, which decreased when the grafting ratio increased (Table 2, Figure 6). The surface modification produced by grafting has a strong effect on the N_2 adsorption at 77 K. For pure silica samples, the BET area was about 140 m^2 g^{-1}. It is in good agreement with the calculated value, assuming nonporous spherical particles of the same diameter D, $S_w = 6/\rho D$ (where ρ is the specific gravity of silica). In all cases, grafting induced a quick decrease in BET area, but a plot of the grafted amount versus the BET area shows (Figure 6) that the effect is far more pronounced with bipyridine-containing compounds (≡**Si-5** and ≡**Si-6**).

For these organosilanes, the first grafted molecule occupies a surface area of 0.36 nm^2, whereas this value is about 0.10 nm^2 for the other groups. This loss in surface area may be explained by the fact that N_2 molecules are repelled from the silica surface by the grafted organosilanes so that they cannot adsorb anymore. The effect appears essentially related to the electronic properties of the organosilanes rather than to the steric one. The surface modification produced by grafting was also demonstrated by the change in the BET C constant. The value of this constant is linked to the heat of adsorption of N_2 on the solid surface.[73] Without grafting, the C value was about 100. After grafting, this value fell below 30 with dipyridine organosilanes but only below 70 for the other functional groups. This shows that grafting decreased the adsorption energy of N_2.

These results show that carefully chosen conditions should be used to limit oligomer grafting on silica nanoparticules. Above all, organic amounts giving different types of coatings are very dependent on the organosilane molecular structure. As shown by Corriu and co-workers,[74] on silsesquioxane materials, structural parameters influence the hydrolytic polymerization of organosilicon precursors. So **5** and **6** with their rigid dipyridyl group are characterized by a lower degree of condensation compared to the more

(73) Brunauer, S.; Hemmett, P. H.; Teller, E. *J. Am. Chem. Soc.* **1938**, *60*, 309.

(74) Cerveau, G.; Corriu, R. J. P.; Lepeytre, C.; Mutin, P. H. *J. Mater. Chem.* **1998**, *8*, 2707.

flexible one, that is, urea molecules giving rise to a relatively high grafting ratio.

Acknowledgment. S.C. thanks MESR for a grant. Authors thank M.-C. Barthélémy for her technical assistance with the nitrogen adsorption isotherm determination.

Supporting Information Available: ^{1}H and $^{13}C\{^{1}H\}$NMR data for compounds 2–6. Tables of selected IR variations of dipyridylsilanes **2**–**6**. Tables of selected DRIFT vibrations of grafted nonohybrids (cm^{-1}). This information is available free of charge via the Internet at http://pubs.acs.org.

CM7019075